Revista AIDIS de Ingeniería y Ciencias Ambientales:
Investigación, desarrollo y práctica. ISSN 0718-378X

http://dx.doi.org/10.22201/iingen.0718378xe.18.1.88930
Vol. 18, No.1, 111-124
Abril 2025

REVISTA AIDIS

de Ingeniería y Ciencias Ambientales: Investigación, desarrollo y práctica.

PHOSPHATE ADSORPTION STUDY EMPLOYING A SYNTHESIZED ACTIVATED CARBON DERIVED FROM BANANA PSEUDOSTEM

Moisés de Souza Luz Faria [1]
Rayra Millene Ribeiro Lima [1]
Rita de Cássia Superbi de Sousa [1]
* Alisson Carraro Borges [2]

Recibido el 7 de junio de 2024. Aceptado el 11 de octubre de 2024

Abstract

In recent years, the application of biomass sources as precursors for various materials has been employed as an alternative for waste reuse. The banana pseudostem, being a lignocellulosic residue generated in huge quantities, has been studied for its reuse possibilities. The use of this biomaterial as a pyrolyzed and activated adsorbent compound is a promising application in wastewater treatment. Phosphorus (P), as a macronutrient, must have its concentration controlled in water bodies, as it contributes to the eutrophication process and causes environmental impact, demanding effective control of its release and removal in wastewater. Although some studies have already applied the banana pseudostem in wastewater treatment, its use for phosphorus removal is still scarce. Therefore, this work aimed to produce and characterize the banana pseudostem activated carbon (BPAC) under specific conditions at 600°C for 90 minutes, through chemical activation with zinc chloride at a ratio of 3:1. The results showed a surface area of 996 $m^2\ g^{-1}$, and the kinetic and adsorption isotherm tests revealed an equilibrium time of 16 hours and a maximum P adsorption capacity of 11.82 mg L^{-1}, respectively. The pseudo-first order kinetics model were better fitted to experimental results, and for the isotherm at 18°C, the Langmuir was better fitted. The pH at the point of zero charge resulted in a value of 7.20, indicating that phosphorus adsorption is better favored below neutrality.

Keywords: *biomass, isotherm, kinetics, zinc chloride, superficial area.*

[1] Departamento de Química, Universidade Federal de Viçosa, Brasil.
[2] Departamento de Engenharia Agrícola, Universidade Federal de Viçosa, Brasil.
** Autor corresponsal:* Departamento de Engenharia Agrícola, Universidade Federal de Viçosa. Campus Universitário, Viçosa, Minas Gerais, 36570-900, Brasil. Email: borges@ufv.br

Revista AIDIS de Ingeniería y Ciencias Ambientales:
Investigación, desarrollo y práctica. ISSN 0718-378X
http://dx.doi.org/10.22201/iingen.0718378xe.18.1.88930
Vol. 18, No.1, 111-124
Abril 2025

Introduction

Agricultural, industrial, and domestic wastewater are the primary sources of high phosphorus concentration, which is an essential nutrient for plant and microorganism growth. Since it is considered an eutotrophic component of water bodies, a series of alternative treatment techniques have been studied, such as precipitation and adsorption for biological degradation, to mitigate its removal and reducing negative impact on the environment. Even low concentration, as low as 2 mg L^{-1}, may enhance the algae growth and reduce the dissolved oxygen, improving the eutrophication process and harming aquatic life (Guo *et al*., 2017). According to normative deliberation COPAM-CERH/MG N° 8 (Minas Gerais, 2022), the maximum total phosphorus limit in freshwater ranges from 0.05 to 0.15 mg L^{-1}, depending on water classification. Following the Council Directive N° 91/271/EEC (Council of the European Communities, 1991), the limits of total phosphorus for urban wastewater disposal vary from 1 to 2 mg L^{-1} in sensitive areas. Zhou *et al*. (2017) reiterated the limit of total phosphorus at 0.5 mg L^{-1} in effluent flow of wastewater treatment plants in China. All these limits values indicate a low tolerance for total phosphorus concentration in water bodies, highlighting the need of able technologies to remove these pollutants from wastewater.

The adsorption process has been studied for decades as an efficient, low-cost, selective and effective method to remove phosphorus from water, reducing its concentration levels. Additionally, this treatment technique promotes the regeneration of the adsorbent and the recovery of the adsorbate through desorption, hence phosphorus cannot be replaced by other resources (Liu & Hu, 2019; Usman *et al*., 2022). Studies have also investigated the potential of activated carbon to remove phosphorus from wastewater using renewable sources such as biomass residues, creating a reuse cycle involving water treatment and residue disposal. For example, Yao *et al*. (2018) used domestic wastewater sludge as a precursor for activated carbon modified with pyrolusite to remove phosphate in batch experiments. Huong *et al*. (2019) developed a low-cost pine cone biomass activated carbon modified with lanthanum chloride and Kumar *et al*. (2010) used coir-pith activated carbon with a sulfuric acid base to verify phosphate removal. Although some studies have explored the activated carbon derived from biomass, their application for phosphorus removal is still limited.

In the context of renewable residues, banana pseudostems have been studied as a promising precursor for activated carbon production and the removal of multiple pollutants from water. Banana is the largest exported and consumed fresh fruit in the world, and Brazil ranks fourth among the world's banana producers (Mappr, 2022). Each banana pseudostem produces one bunch of bananas, and when it becomes unproductive, it is cut down while a new pseudostem grows (Fernandes *et al*., 2013). It is estimated that each ton of bananas generates 4 tons of residues, with 3 tons coming from the pseudostem alone (Abdullah *et al*., 2023). Hence, a massive quantity of waste is generated, many studies have explored this residue as an activated carbon precursor for wastewater treatment. Examples include the removal of dyes such as methylene

Revista AIDIS de Ingeniería y Ciencias Ambientales:
Investigación, desarrollo y práctica. ISSN 0718-378X
http://dx.doi.org/10.22201/iingen.0718378xe.18.1.88930
Vol. 18, No.1, 111-124
Abril 2025

blue (Jiang *et al*., 2022; Silva *et al*., 2021), indigo carmine (Debina *et al*., 2020), Crystal violet (Baharim *et al*., 2023), as well as the removal of physicochemical parameters such as color and chemical oxygen demand from leachate (Ghani *et al*., 2017).

In this study, the banana pseudostem was modified to use as a biomass for activated carbon production using zinc chloride ($ZnCl_2$) as a chemical impregnant for activation. A series of batch adsorption tests were conducted to determine the time of equilibrium during adsorption kinetics, and the maximum quantity of phosphate adsorbed per gram of adsorbent. Additionally, the surface area of the BPAC was calculated to determine its total area, and a pH test was conducted to identify the optimal pH range for phosphorus removal.

Materials and methods

Banana Pseudostem Activated Carbon (BPAC) production

The activated carbon was produced using banana pseudostem (*Musa* spp.) as a precursor according to Ghani *et al*. (2017). After fruit harvesting, the biomass was collected from banana trees in the Experimental Waste Treatment Area in the Federal University of Viçosa, Brazil. The biomass was fragmented into small pieces approximately 3 to 5 cm in length, and dried under sunlight for 7 days. Then, it was placed in an air-forced oven (Marconi, MA035) for an additional 2 days to remove residual water, at 65°C. The dried material was ground, using a compact processor (Philco, PH 900 Turbo), and the material that passed through a 35-mesh sieve was stored in an airtight container for subsequent experiments.

Four steps were employed in BPAC production: impregnation, pyrolysis, washing, and drying. Impregnation involved using a fixed precursor mass of 15 g in a 100 mL ceramic crucible, with a 3:1 mass ratio of zinc chloride (Neon, 97% analytical grade) as a chemical activator. This indicates that 3 grams of anhydrous zinc chloride were used for every gram of biomass. The impregnant was diluted in deionized water for better impregnation. Approximately 50 mL of zinc chloride solution was mixed and thoroughly stirred into the precursor inside the ceramic crucible with a glass rod, until the mixture presented a homogeneous and high viscous aspect. Subsequently, the mixture was placed in an oven (Orion, 515) at 105°C for 24 hours to evaporate excess water and initiate the first depolymerization process. During this time of impregnation, the crucible was kept static.

After removing the impregnated biomass from the oven, it was stored in a desiccator until achieving room temperature, and then the crucible was covered with a ceramic lid and conducted into a muffle furnace (SP Labor, SP-1200). The pyrolysis was performed at 600°C, during 90 minutes at 10°C min^{-1} heating rate. Subsequently, the furnace was turned off, and after 4 hours, the crucible was removed and retained in a desiccator until it reached room temperature. The waiting time (after the furnace was turned off) was used for sample temperature reduction and to prevent

Revista AIDIS de Ingeniería y Ciencias Ambientales:
Investigación, desarrollo y práctica. ISSN 0718-378X
http://dx.doi.org/10.22201/iingen.0718378xe.18.1.88930
Vol. 18, No.1, 111-124
Abril 2025

carbon oxidation during crucible movement, as well as for the completion of smoke formation during volatile matter emission.

The BPAC was retired from the crucible with a spatula and transferred into a mortar. As there was a residual $ZnCl_2$ in the pyrolyzed material, it exhibited a hard aspect. To facilitate the washing process, BPAC was soaked in a 0.1 mol L^{-1} HCl solution, and then ground with a mortar into small granules. The acid-soaked BPAC mixture was stirred for 1 hour and then washed with hot deionized water (approximately 85°C) using a vacuum pump-filter system (0.45 µm). This process was repeated until the pH of the supernatant was equal to the water pH used for washing. The pH was measured when supernatant achieved room temperature. The wet BPAC was placed in an air-forced oven at 65°C for 2 days, then ground with a mortar, and the material that passed through a 35-mesh sieve was stored in an airtight container for the next experiments.

Point of zero charge (pH_{pzc})

The pH_{pzc} was determined according to Akkari *et al*. (2023). In this method, 50 mL of a 0.1 mol L^{-1} NaCl solution was prepared in conical flasks, and the pH value was adjusted varying from 2.00 to 12.00 in 2 units increments, using 0.1 mol L^{-1} NaOH or 0.1 mol L^{-1} HCl solutions. A quantity of 0.15 g of BPAC was placed in each flask and shaken at 120 rpm for one day. After that, the samples were filtered with 0.45 µm, and pH_{final} values from filtered supernatant were measured. The pH_{final} x $pH_{initial}$ and bisector curves were plotted in the same graph. The intersection point between pH_{final} x pH_{inital} and bisector curves determined the pH_{pzc}.

N_2 adsorption-desorption analyses

To determine the surface area, the N_2 adsorption-desorption analysis was conducted. A quantity of 0.5 g of BPAC powder was used in this analyze, employing a surface area and porosity analyzer (TriStar, II3020). First, the sample was placed in a glass bulb and degassed for 3 hours, to remove moisture and other volatile components. After degassing, the glass bulb was transferred into a liquid nitrogen (77 K) bath for a surface area calculus.

Adsorption kinetics

Adsorption kinetics were conducted using a fixed phosphorus initial concentration of 400 mg L^{-1}. 0.1 g mass of adsorbent was placed in conical flasks and mixed with 50 mL of phosphorus solution. A time range (0.5, 2, 4, 8, 16, 24, 40 and 48 h) was defined for detecting the remaining phosphorus in the solution. This experiment was conducted in duplicate. Phosphorus was detected using the ascorbic acid method in liquid, as preconized in Standard Methods for Examination of Water and Wastewater (APHA, 2023), using a spectrophotometer (Hach, DR6000) at 880 nm wavelength. A 400 mg $P\text{-}PO_4^{-3}$ L^{-1} stock solution was prepared using KH_2PO_4 salt. Based on a mass balance, the quantity of adsorbed phosphorus in BPAC was determined by Equation (1). The pseudo-first and pseudo-second order kinetics models were fitted to experimental results according to the Equations (2) and (3), respectively.

Revista AIDIS de Ingeniería y Ciencias Ambientales:
Investigación, desarrollo y práctica. ISSN 0718-378X
http://dx.doi.org/10.22201/iingen.0718378xe.18.1.88930
Vol. 18, No.1, 111-124
Abril 2025

$$q = \frac{(c_0 - c)V}{m} \quad \text{Equation (1)}$$

$$q_t = q_e(1 - e^{k_1 t}) \quad \text{Equation (2)}$$

$$q_t = \frac{k_2 {q_e}^2 t}{1 + k_2 q_e t} \quad \text{Equation (3)}$$

where q is the adsorbate quantity per gram of BPAC, (mg g^{-1}), c_0 is the initial phosphorus concentration in solution, (mg L^{-1}), c is the phosphorus concentration in solution, (mg L^{-1}), V is the sample volume, (L), m is the adsorbent mass in the flask, (g), k_1 is the adsorption rate pseudo-first order constant, (h^{-1}), k_2 is the adsorption rate pseudo-second order constant, (g mg^{-1} h^{-1}), q_e is the adsorbed quantity per gram of adsorbent in the equilibrium, (mg g^{-1}), q_t is the adsorbed quantity per gram of adsorbent in an instant t (mg g^{-1}).

The intra-particle diffusion was conducted to identify the mechanism in which adsorbate moves from solution to the surface of the adsorbate. The Equation (4) gives the expression to this model.

$$q_t = k_p t^{0.5} + C \quad \text{Equation (4)}$$

where q_t is the quantity of adsorbate adsorbed per gram of adsorbent in a given time t, (mg g^{-1}), k_p is the intra-particle diffusion rate constant, (mg g^{-1} $h^{-0.5}$), t is the time, (h), and C is the constant which is related to thickness of boundary layer, (mg g^{-1}).

Adsorption Isotherm

The adsorption isotherm was conducted over the time of equilibrium found in kinetics adsorption tests with 8 varying points of adsorbate concentration (5, 10, 20, 30, 50, 100, 300, 400 mg L^{-1}). While the main purpose of kinetics was to find the equilibrium time, the isotherm aims to discover the capacity of BPAC in adsorbing phosphorus. A q_e x c_e curve was plotted, and Langmuir and Freundlich models were adjusted to experimental results as described in Equations (5) and (6).

$$q_e = \frac{q_{max} K_L c_e}{1 + K_L c_e} \quad \text{Equation (5)}$$

$$q_e = K_F {c_e}^{1/n} \quad \text{Equation (6)}$$

where q_e is the quantity of adsorbed solute per gram of adsorbent in the equilibrium, (mg g^{-1}), K_L is the adsorbate-adsorbent interaction constant, (L mg^{-1}), c_e is the adsorbate concentration in solution at the equilibrium, (mg L^{-1}), K_F is the Freundlich adsorption capacity constant, ($mg^{1-(1/n)}$ g^{-1} $L^{1/n}$), n is a dimensionless constant value related to the BPAC surface heterogeneity.

Revista AIDIS de Ingeniería y Ciencias Ambientales:
Investigación, desarrollo y práctica. ISSN 0718-378X
http://dx.doi.org/10.22201/iingen.0718378xe.18.1.88930
Vol. 18, No.1, 111-124
Abril 2025

Results and discussion

Point of zero charge (pH_{pzc}) and S_{BET}

The point of zero charge (pH_{pzc}) indicates the pH value at which the net charge on the activated carbon surface is zero. When pH values are below the pH_{pzc}, the surface charge is positive due to the protonation effect caused by excess H^+ ions, which benefits anion adsorption. In contrast, when pH values are above the pH_{pzc}, the surface charge is negative due to deprotonation, thus facilitating cation adsorption (Akkari *et al*., 2023; Nascimento *et al*., 2014). Therefore, this characterization provides an important method for determining an optimal pH range for interaction between adsorbate and adsorbent (Bagali *et al*., 2017). The result for BPAC is shown in Figure 1, where the intersection point of the pH_{final} vs. $pH_{initial}$ curve and the bisector indicates a pH_{pzc} of 7.20. Thus, since electrostatic attraction increases, phosphorus adsorption is favored when pH < 7.20. The S_{BET} result showed a surface area of 996 $m^2\ g^{-1}$, which demonstrates a high surface value for adsorption. It is important, though, to remind that not necessarily all this area is provided of active sites for phosphorus adsorption (Nascimento *et al*., 2014).

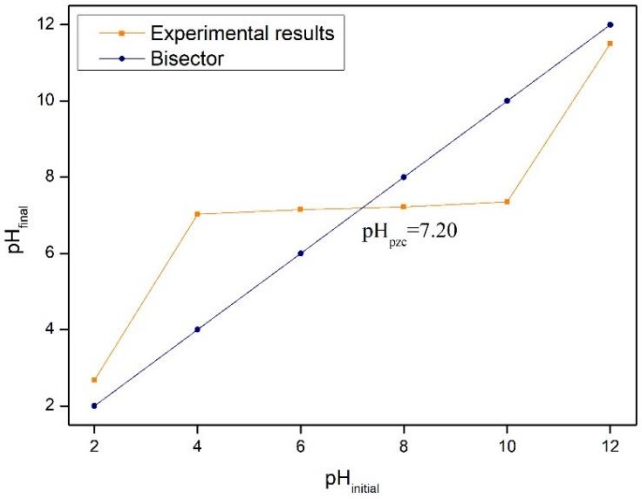

Figure 1. Variation of pH for the determination of BPAC point of zero charge

Kinetics Adsorption

The kinetics experiment results revealed an equilibrium time of approximately 16 h and q_e value of 10.70 mg g^{-1}. The experimental results were fitted to both pseudo-first and pseudo-second order. The results showed a R^2 value of 0.94924 for pseudo-second order model (not shown here) and 0.96861 for pseudo-first order reaction. Figure 3 (a) displays the experimental results with pseudo-first order fitting, along with the resulting kinetics equation for phosphorus adsorption. For a validation of the model, besides RMSE value, a q residue x q observed values and q predicted

Revista AIDIS de Ingeniería y Ciencias Ambientales:
Investigación, desarrollo y práctica. ISSN 0718-378X
http://dx.doi.org/10.22201/iingen.0718378xe.18.1.88930
Vol. 18, No.1, 111-124
Abril 2025

x q observed were plotted, as it follows in Figure 2, (a) and (b) respectively. It is possible to observe that q_{res} x q_{obs} and q_{pred} x q_{obs} show a good model fitting, once the residues are aleatory distributed and there is a higher correlation between the observed and predicted values.

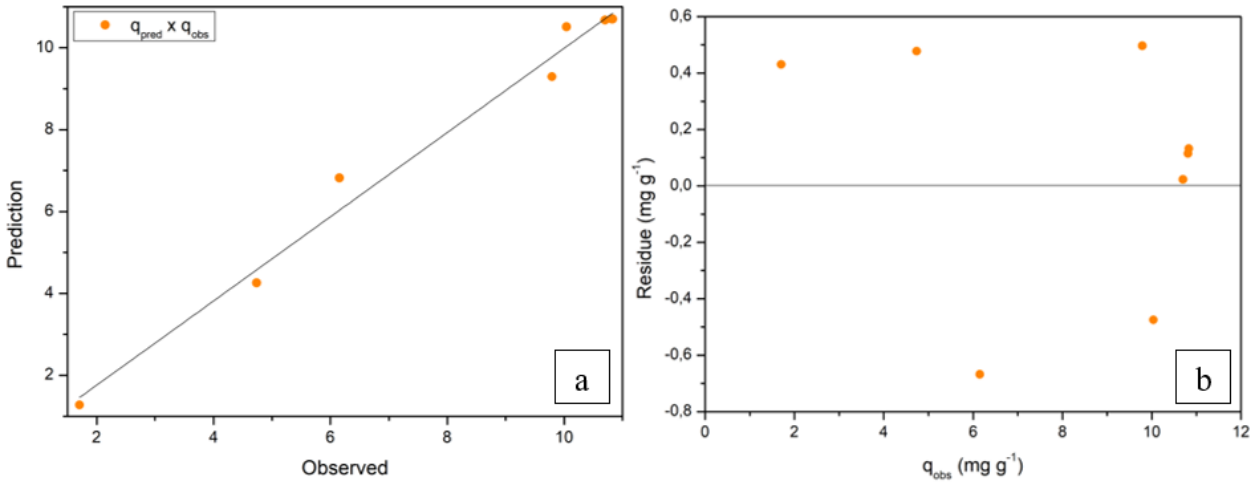

Figure 2. (a) Model prediction results versus observed values. (b) residue values versus observed values of q. All the axes in both graphs are disposed in mg g^{-1} units

The proposed models do not describe a diffusion mechanism for adsorption, then the intra-particle diffusion model was executed by plotting a q_t x $t^{0.5}$ graph, as shown in Figure 3 (b). The q_t x $t_{0.5}$ graph is subdivided into three stages, with higher (1), medium (2), and lower slopes (3). This indicates that two or more steps occurred in the adsorption process. If the first one (higher slope) generates a layer that intercepts the origin, then intra-particle diffusion is the only process involved in the adsorption (Nascimento *et al*., 2014). For this experiment, the intercept value was -0.56783, and although it is close to zero, it corresponds to the possibility of external mass transfer or even a chemical reaction that may have occurred in stage 1. The second stage indicates a gradual adsorption rate. The third stage is characterized by lower adsorption rates, and intra-particle diffusion ceases.

According to Figure 3 (b), there is an inflection point at the beginning of medium slope layer. Then, the adsorption process occurs in external diffusion and mild diffusion (which starts to happen in medium slope). The external diffusion corresponds to the adsorbate migration from the solution to the solution layers around the adsorbent surface (Yuan *et al*., 2021). The reasons for the profile from intra-particle diffusion found in this study are that the available pores for diffusion were filled or became smaller, and the electrostatic repulsion in the BPAC increased (Wang *et al*., 2012). Table 1 shows a comparative result of experimental studies using activated carbon for phosphate removal, where the results showed a q_e range varying from 1.5 to 12.18 mg g^{-1}.

Revista AIDIS de Ingeniería y Ciencias Ambientales:
Investigación, desarrollo y práctica. ISSN 0718-378X
http://dx.doi.org/10.22201/iingen.0718378xe.18.1.88930
Vol. 18, No.1, 111-124
Abril 2025

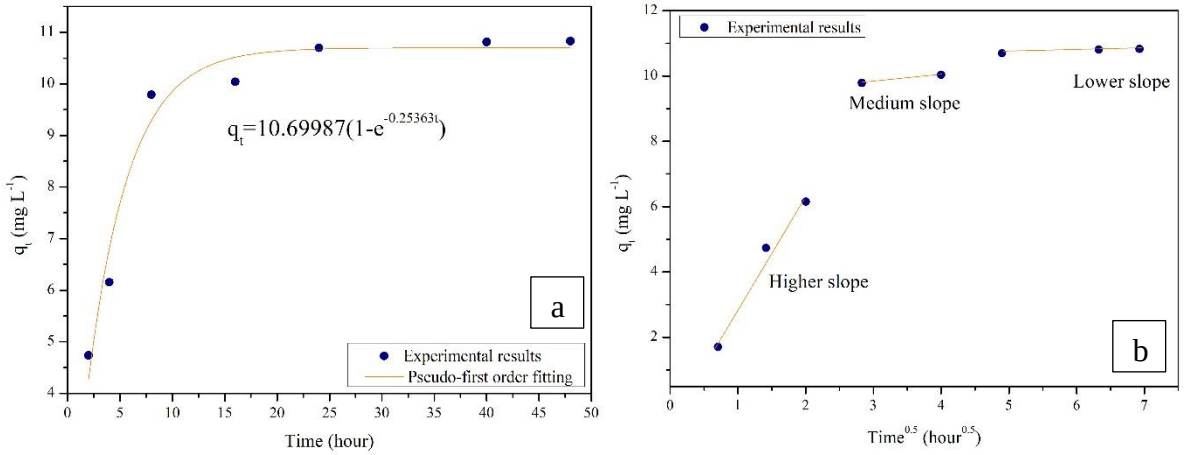

Figure 3. (a) kinetic experiment with better fitting model of pseudo-first order. (b) intra-particle diffusion fitting model with 3 stages of adsorption

Table 1. Experimental kinetics studies using activated carbon for phosphorus removal

q_e (mg g^{-1})	t_e (h)	Temperature (°C)	Activated carbon origin	Reference
6.97	24	25	Pinewood biochar impregnated with $ZnCl_2$	Biswas *et al*. (2023)
≈ 1.5	≈ 250	25	Commercial granular activated carbon impregnated with iron oxide	Braun *et al*. (2019)
0.7307	30	25	Sheep dung impregnated with La and Mg	Chen *et al*. (2024)
≈ 0.014 – 0.017	≈ 5	25±2	Granular activated carbon mixed with limestone	Hussain *et al*. (2011)
1.44	10-12	25	Granular activated carbon impregnated with ferrihydrite	Mahardika *et al*. (2018)
3.289	2	30	Commercial activated carbon	Mor *et al*. (2017)
1.452	≈ 1.3	35	Coconut fiber residues impregnated with $ZnCl_2$	Namasivayam & Sangeetha (2004)
2.58	3	19±1	Commercial powder-activated carbon	Ouakouak & Youcef (2016)
10.21	4.5	35	Commercial activated carbon modified with HNO_3 and doped with iron oxide.	Wang *et al*. (2012)
8.99	5	Room temperature	Digestate from anaerobic digestion impregnated with KOH	Zhang *et al*. (2022)
12.18	24	Room temperature	Activated carbon fiber doped with ferric oxide	Zhou *et al*. (2012)
10.70	16	18±2	Banana pseudostem impregnated with $ZnCl_2$	This study

Revista AIDIS de Ingeniería y Ciencias Ambientales:
Investigación, desarrollo y práctica. ISSN 0718-378X
http://dx.doi.org/10.22201/iingen.0718378xe.18.1.88930
Vol. 18, No.1, 111-124
Abril 2025

BPAC removed the greater quantity of phosphorus at the lower temperature. Wang *et al*. (2012) also obtained a value close to q_e in a shorter time, and although less time may be interesting, four of the related studies still exhibit an equilibrium time greater than 16 hours. For the seven remaining comparison studies, it was exhibited an equilibrium time below 16 hours, but they showed lower q_e values than BPAC. The adsorption rate and, consequently, the equilibrium time, are strongly affected by adsorbent and solution properties such as pore size distribution, surface area, pH, ionic strength, and adsorbate concentration (Nascimento *et al*., 2014). The statistical parameters for pseudo-first order and intra-particle diffusion for the higher slope are given in Table 2.

Table 2. Adsorption kinetics parameters for BPAC.

	Pseudo-first order				Intra-particle diffusion (3 initial data points)			
	q_e (mg g^{-1})	k_1 (h^{-1})	R_{adj}^2	Root Mean Squared Error (mg g^{-1})	k_p (mg g^{-1} $h^{-0.5}$)	C (mg g^{-1})	R_{adj}^2	Root Mean Squared Error (mg g^{-1})
Results	10.69987	0.25363	0.96233	0.48547	3.46789	-0.56783	0.95401	0.23737
Standard deviation	0.24878	0.02461	-	-	0.53215	0.7833	-	-

Isotherm adsorption

The batch isotherm study was executed in 20°C, with a pH solution value of 4.50 (stock solution of 400 mg P L^{-1}) during 16 h, as it was the equilibrium time found in kinetics. The dilution from stock solution did not affect the value of pH in the concentration range used in the isotherm experiment, and all values ranged from 4.18 – 4.52, which is a great value for phosphorus removal, according to pH_{pzc} (7.20). The experimental data were fitted to Langmuir and Freundlich isotherms models, in which the statistical results are given in Table 3. The difference between the values of Root Mean Squared Error (RMSE) shows that the experimental data better fits to Langmuir model with a q_{max} of 11.82 mg g^{-1} of P, which indicates the adsorption of phosphorus was a monolayer adsorption process and the BPAC has a uniform site energy distribution. The R_L value is an indicative parameter for the degree of development of the adsorption process, which can be related to a separation factor, given by Equation (7).

$$R_L = \frac{1}{1+K_L c_0} \quad \text{(Equation 7)}$$

where c_0 corresponds to the initial concentration of adsorbate in fluid phase, (mg L^{-1}), which for this study is 5.00 mg L^{-1}.

Revista AIDIS de Ingeniería y Ciencias Ambientales:
Investigación, desarrollo y práctica. ISSN 0718-378X
http://dx.doi.org/10.22201/iingen.0718378xe.18.1.88930
Vol. 18, No.1, 111-124
Abril 2025

Proceeding with the substitution in Equation (7), it is found a R_L value of approximately 0.70. When the $0<R_L<1$, the adsorption is favorable and the adsorbate prefers the solid phase than the fluid one (Nascimento *et al.*, 2014). Figure 4 indicates isotherm fitting where the experimental results can be observed to be more aligned with the Langmuir model than the Freundlich.

Table 3. Statistical parameters for adsorption isotherm models for BPAC

	Langmuir					Freundlich				
	q_{max} (mg g^{-1})	K_L (L mg^{-1})	R^2	R_{adj}^2	RMSE (mg g^{-1})	K_F ($mg^{1-(1/n)}$ g^{-1} $L^{1/n}$)	n	R^2	R_{adj}^2	RMSE (mg g^{-1})
Results	11.81811	0.08416	0.92986	0.91711	0.92978	4.01879	5.40173	0.66641	0.61082	2.01474
Standard deviation	0.62656	0.01956	-	-		1.14129	1.74735	-	-	-

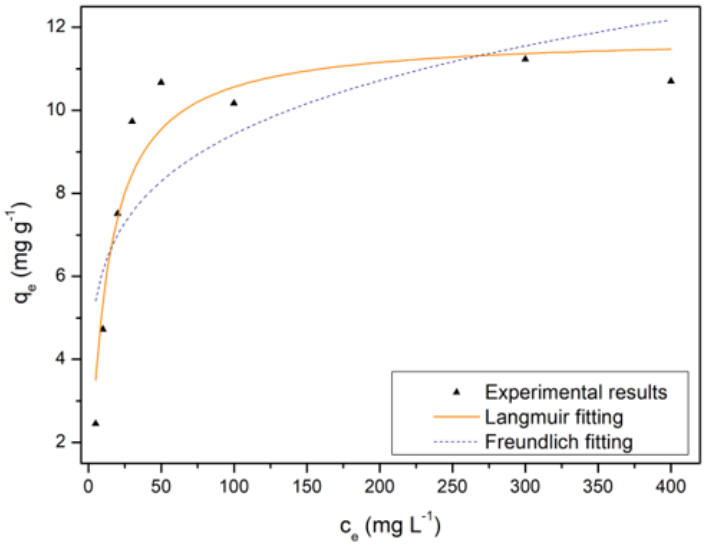

Figure 4. Isotherm models fitting in contrast with experimental results.

The large-scale production of activated carbon can be costly, which hinders its scalability, making economic and environmental analysis necessary. BPAC has proven viable in terms of its properties such as high surface area, with a relatively quick production cycle (5.5 hours from the start of pyrolysis to the removal of the material from the furnace). Phosphorus removal rates were

Revista AIDIS de Ingeniería y Ciencias Ambientales:
Investigación, desarrollo y práctica. ISSN 0718-378X
http://dx.doi.org/10.22201/iingen.0718378xe.18.1.88930
Vol. 18, No.1, 111-124
Abril 2025

around 98% for an initial concentration of 5 mg L^{-1} and 94% for 10 mg L^{-1} (near value to the q_{max}), with an average BPAC production yield of 36% (dry basis). These results indicate good applicability of BPAC for phosphorus removal.

Steps like sun drying could be replaced by oven drying, which is already used to eliminate residual moisture, thus reducing the material preparation time. The production steps involve costs related to fragmentation, drying, and impregnation of banana pseudostem, processes already common in the production of activated carbons from biomass precursors. Costs related to the chemical reagent, energy for pyrolysis, and material washing should also be considered in the development of a biochar with high surface area and adsorptive capacity. Additional steps, especially regarding the treatment and disposal of wash water containing zinc residues, can be mitigated by implementing coagulation-flocculation or caustic precipitation processes (Lim *et al*., 2021).

One advantage of this biochar production method is that it results in a composite with a high surface area made in an atmosphere with low oxygen concentration, eliminating the need for an inert atmosphere (usually N_2) and specific reactors. The banana pseudostem can be sourced in large quantities from local plantations continuously, due to the high global production for bananas and favorable climatic conditions in tropical regions. Logistics issues should be further investigated, particularly regarding transportation of the material to processing facilities. However, other pseudostem processing activities already occur through commercial agreements between industry and banana cultivars (Badanayak *et al*., 2023). The operating temperature of 600°C can also offer advantages in terms of energy consumption and scalability, since pyrolysis temperatures typically range from 600°C to 1000°C (Chew *et al*., 2023). Considering these factors, large-scale production of this adsorbent holds significant potential for the cyclic reuse of biomaterials.

Conclusion

The BPAC showed a good response in phosphorus removal at the tested temperature and pH values when compared to other renewable biomass precursors. This indicates that the conditions for BPAC production provide a promising source of renewable material for removing this macronutrient from water and wastewater. The experimental results showed that the pyrolysis temperature (600°C) aligned with time of pyrolysis (90 min) and $ZnCl_2$ impregnation ratio of 3:1 were successfully employed for this application. For future studies, it is recommended that new isotherms at different temperatures be employed to better investigate the influence of this variable on the maximum removal capacity. Additionally, the high S_{BET} area (996 $m^2\ g^{-1}$) may indicate potential for removing other pollutants, such as toxic metals, dyes, antibiotics, and nutrients from wastewater, being necessary a complementary analysis of functional groups in the BPAC surface.

Revista AIDIS de Ingeniería y Ciencias Ambientales:
Investigación, desarrollo y práctica. ISSN 0718-378X
http://dx.doi.org/10.22201/iingen.0718378xe.18.1.88930
Vol. 18, No.1, 111-124
Abril 2025

Acknowledge

This study was partially funded by the Coordination for the Improvement of Higher Education Personnel - Brazil (CAPES) under Finance Code 001, and the Minas Gerais Research Foundation (FAPEMIG), grant number APQ-03626-22.

References

Abdullah, N., Mohd Taib, R., Mohamad Aziz, N. S., Omar, M. R., Md Disa, N. (2023). Banana pseudo-stem biochar derived from slow and fast pyrolysis process. *Heliyon*, **9**(1). https://doi.org/10.1016/j.heliyon.2023.e12940

Akkari, I., Graba, Z., Bezzi, N., Merzeg, F. A., Bait, N., Ferhati, A. (2023). Raw pomegranate peel as promise efficient biosorbent for the removal of Basic Red 46 dye: equilibrium, kinetic, and thermodynamic studies. *Biomass Conversion and Biorefinery*, **13**(9), 8047–8060. https://doi.org/10.1007/s13399-021-01620-9

APHA, AWWA, WEF. (2023). *Standard Methods for the Examination of Water and Wastewater*, 24th ed., APHA (American Public Health Association), USA

Badanayak, P., Jose, S., Bose, G. (2023). Banana pseudostem fiber: A critical review on fiber extraction, characterization, and surface modification. *Journal of Natural Fibers*, **20**(1). https://doi.org/10.1080/15440478.2023.2168821

Bagali, S. S., Gowrishankar, B. S., Roy, A. S. (2017). Optimization, Kinetics, and Equilibrium Studies on the Removal of Lead(II) from an Aqueous Solution Using Banana Pseudostem as an Adsorbent. *Engineering*, **3**(3), 409–415. https://doi.org/10.1016/J.ENG.2017.03.024

Baharim, N. H., Sjahrir, F., Taib, R. M., Idris, N., Daud, T. A. T. (2023). Removal of Crystal Violet from Aqueous Solution using Post-Treated Activation Biochar Derived from Banana Pseudo Stem. *Chemical Engineering Transactions*, **98**, 45–50. https://doi.org/10.3303/CET2398008

Biswas, B., Rahman, T., Sakhakarmy, M., Jahromi, H., Eisa, M., Baltrusaitis, J., Lamba, J., Torbert, A., Adhikari, S. (2023). Phosphorus adsorption using chemical and metal chloride activated biochars: Isotherms, kinetics and mechanism study. *Heliyon*, ***9***(9), e19830. https://doi.org/10.1016/j.heliyon.2023.e19830

Braun, J. C. A., Borba, C. E., Godinho, M., Perondi, D., Schontag, J. M., Wenzel, B. M. (2019). Phosphorus adsorption in Fe-loaded activated carbon: Two-site monolayer equilibrium model and phenomenological kinetic description. *Chemical Engineering Journal*, **361**, 751–763. https://doi.org/10.1016/j.cej.2018.12.073

Chen, J., Chen, Z., Song, Z., Cao, S., Li, X., Wang, Y., Zhan, Z., Du, M., Teng, D., Lv, D., Shao, D. (2024). Preparation of La/Mg modified sheep dung activated carbon and its adsorption characteristics for phosphorus in wastewater. *Desalination and Water Treatment*, **317**, 100013. https://doi.org/10.1016/j.dwt.2024.100013

Chew, T. W., H'Ng, P. S., Luqman Chuah Abdullah, B. C. T. G., Chin, K. L., Lee, C. L., Mohd Nor Hafizuddin, B. M. S., TaungMai, L. (2023). A Review of Bio-Based Activated Carbon Properties Produced from Different Activating Chemicals during Chemicals Activation Process on Biomass and Its Potential for Malaysia. *Materials*, **16**(23), 7365. https://doi.org/10.3390/ma16237365

COPAM-CERH/MG, Conselho Estadual de Política Ambiental e Conselho Estadual de Recursos Hídricos de Minas Gerais. (2022). Deliberação Normativa Conjunta COPAM-CERH/MG Nº 8. *Diário do Executivo – Minas Gerais*, 2 de dezembro de 2022. Avaliable at: https://www.siam.mg.gov.br/sla/download.pdf?idNorma=56521

Council of the European Communities. (1991). Council Directive 91/271/EEC of 21 May 1991 concerning urban waste water treatment. *Official Journal of the European Communities, L135*, 40-52. Avaliable at: https://eur-lex.europa.eu/legal-content/EN/TXT/PDF/?uri=OJ:L:1991:135:FULL

Debina, B., Eric, S. N., Fotio, D., Arnaud, K. T., Lemankreo, D.-Y., Rahman, A. N. (2020). Adsorption of Indigo Carmine Dye by Composite Activated Carbons Prepared from Plastic Waste (PET) and Banana Pseudo Stem. *Journal of Materials Science and Chemical Engineering*, **08**(12), 39–55. https://doi.org/10.4236/msce.2020.812004

Revista AIDIS de Ingeniería y Ciencias Ambientales:
Investigación, desarrollo y práctica. ISSN 0718-378X
http://dx.doi.org/10.22201/iingen.0718378xe.18.1.88930
Vol. 18, No.1, 111-124
Abril 2025

Fernandes, E. R. K., Marangoni, C., Souza, O., Sellin, N. (2013). Thermochemical characterization of banana leaves as a potential energy source. *Energy Conversion and Management*, **75**, 603–608. https://doi.org/10.1016/j.enconman.2013.08.008

Ghani, Z. A., Yusoff, M. S., Zaman, N. Q., Zamri, M. F. M. A., Andas, J. (2017). Optimization of preparation conditions for activated carbon from banana pseudo-stem using response surface methodology on removal of color and COD from landfill leachate. *Waste Management*, **62**, 177–187. https://doi.org/10.1016/j.wasman.2017.02.026

Guo, Z., Li, J., Guo, Z., Guo, Q., Zhu, B. (2017). Phosphorus removal from aqueous solution in parent and aluminum-modified eggshells: thermodynamics and kinetics, adsorption mechanism, and diffusion process. *Environmental Science and Pollution Research*, **24**(16), 14525–14536. https://doi.org/10.1007/s11356-017-9072-8

Huong, P. T., Jitae, K., Giang, B. L., Nguyen, T. D., Thang, P. Q. (2019). Novel lanthanum-modified activated carbon derived from pine cone biomass as ecofriendly bio-sorbent for removal of phosphate and nitrate in wastewater. *Rendiconti Lincei. Scienze Fisiche e Naturali*, **30**(3), 637–647. https://doi.org/10.1007/s12210-019-00827-3

Hussain, S., Aziz, H. A., Isa, M. H., Ahmad, A., Van Leeuwen, J., Zou, L., Beecham, S., Umar, M. (2011). Orthophosphate removal from domestic wastewater using limestone and granular activated carbon. *Desalination*, **271**(1–3), 265–272. https://doi.org/10.1016/j.desal.2010.12.046

Jiang, F., Cao, D., Hu, S., Wang, Y., Zhang, Y., Huang, X., Zhao, H., Wu, C., Li, J., Ding, Y., Liu, K. (2022). High-pressure carbon dioxide-hydrothermal enhance yield and methylene blue adsorption performance of banana pseudo-stem activated carbon. *Bioresource Technology*, **354**, 127137. https://doi.org/10.1016/j.biortech.2022.127137

Kumar, P., Sudha, S., Chand, S., Srivastava, V. C. (2010). Phosphate Removal from Aqueous Solution Using Coir-Pith Activated Carbon. *Separation Science and Technology*, **45**(10), 1463–1470. https://doi.org/10.1080/01496395.2010.485604

Lim, S. S., Fontmorin, J.-M., Pham, H. T., Milner, E., Abdul, P. M., Scott, K., Head, I., Yu, E. H. (2021). Zinc removal and recovery from industrial wastewater with a microbial fuel cell: Experimental investigation and theoretical prediction. *Science of The Total Environment*, *776*, 145934. https://doi.org/10.1016/j.scitotenv.2021.145934

Liu, Y., Hu, X. (2019). Kinetics and Thermodynamics of Efficient Phosphorus Removal by a Composite Fiber. *Applied Sciences*, **9**(11), 2220. https://doi.org/10.3390/app9112220

Mahardika, D., Park, H.-S., Choo, K.-H. (2018). Ferrihydrite-impregnated granular activated carbon (FH@GAC) for efficient phosphorus removal from wastewater secondary effluent. *Chemosphere*, **207**, 527–533. https://doi.org/10.1016/j.chemosphere.2018.05.124

Mappr. (2022). *Top 10 Largest Banana Producing Countries*. Access at 09 May 2024. Avaliabe at: https://www.mappr.co/largest-banana-producing-countries/

Mor, S., Chhoden, K., Negi, P., Ravindra, K. (2017). Utilization of nano-alumina and activated charcoal for phosphate removal from wastewater. *Environmental Nanotechnology, Monitoring Management*, **7**, 15–23. https://doi.org/10.1016/j.enmm.2016.11.006

Namasivayam, C., Sangeetha, D. (2004). Equilibrium and kinetic studies of adsorption of phosphate onto ZnCl2 activated coir pith carbon. *Journal of Colloid and Interface Science*, **280**(2), 359–365. https://doi.org/10.1016/j.jcis.2004.08.015

Nascimento, R. F. do, Lima, A. C. A. de, Vidal, C. B., Melo, D. de Q., Raulino, G. S. C. (2014). *Adsorção: Aspectos teóricos e aplicações ambientais*. Imprensa Universitária da Universidade Federal do Ceará.

Ouakouak, A. K., Youcef, L. (2016). Phosphates Removal by Activated Carbon. *Sensor Letters*, **14**(6), 600–605. https://doi.org/10.1166/sl.2016.3664

Silva, M. C., Spessato, L., Silva, T. L., Lopes, G. K. P., Zanella, H. G., Yokoyama, J. T. C., Cazetta, A. L., Almeida, V. C. (2021). H3PO4–activated carbon fibers of high surface area from banana tree pseudo-stem fibers: Adsorption studies of methylene blue dye in batch and fixed bed systems. *Journal of Molecular Liquids*, **324**, 114771. https://doi.org/10.1016/j.molliq.2020.114771

Revista AIDIS de Ingeniería y Ciencias Ambientales:
Investigación, desarrollo y práctica. ISSN 0718-378X
http://dx.doi.org/10.22201/iingen.0718378xe.18.1.88930
Vol. 18, No.1, 111-124
Abril 2025

Usman, M. O., Aturagaba, G., Ntale, M., Nyakairu, G. W. (2022). A review of adsorption techniques for removal of phosphates from wastewater. *Water Science and Technology*, **86**(12), 3113–3132. https://doi.org/10.2166/wst.2022.382

Wang, Z., Nie, E., Li, J., Yang, M., Zhao, Y., Luo, X., Zheng, Z. (2012). Equilibrium and kinetics of adsorption of phosphate onto iron-doped activated carbon. *Environmental Science and Pollution Research*, **19**(7), 2908–2917. https://doi.org/10.1007/s11356-012-0799-y

Yao, S., Wang, M., Liu, J., Tang, S., Chen, H., Guo, T., Yang, G., Chen, Y. (2018). Removal of phosphate from aqueous solution by sewage sludge-based activated carbon loaded with pyrolusite. *Journal of Water Reuse and Desalination*, **8**(2), 192–201. https://doi.org/10.2166/wrd.2017.054

Yuan, J., Zhu, Y., Wang, J., Liu, Z., He, M., Zhang, T., Li, P., Qiu, F. (2021). Facile Modification of Biochar Derived from Agricultural Straw Waste with Effective Adsorption and Removal of Phosphorus from Domestic Sewage. *Journal of Inorganic and Organometallic Polymers and Materials*, **31**(9), 3867–3879. https://doi.org/10.1007/s10904-021-01992-5

Zhang, C., Sun, S., Xu, S., Johnston, C., Wu, C. (2022). Phosphorus Removal from Dirty Farmyard Water by Activated Anaerobic-Digestion-Derived Biochar. *Industrial Engineering Chemistry Research*, 62(45), 19216-19224. https://doi.org/10.1016/j.bej.2022.108679

Zhou, K., Barjenbruch, M., Kabbe, C., Inical, G., Remy, C. (2017). Phosphorus recovery from municipal and fertilizer wastewater: China's potential and perspective. *Journal of Environmental Sciences*. **52**, 151-159, http://dx.doi.org/10.1016/j.jes.2016.04.010

Zhou, Q., Wang, X., Liu, J., Zhang, L. (2012). Phosphorus removal from wastewater using nano-particulates of hydrated ferric oxide doped activated carbon fiber prepared by Sol–Gel method. *Chemical Engineering Journal*, *200–202*, 619–626. https://doi.org/10.1016/j.cej.2012.06.123